Kinetics of Oxygen Atom Transfer in an Analogue Reaction System of the Molybdenum Oxotransferases

Brian E. Schultz[1] **and R. H. Holm***

Department of Chemistry, Harvard University, Cambridge, Massachusetts 02138

Received March 31, 1993®

A newly developed analogue reaction system of the molybdenum oxotransferases, MoO_2(tBuL-NS)$_2$ (**2**) + X ⇄ MoO(tBuL-NS)$_2$ (**3**) + XO (tBuL-NS = bis(4-tert-butylphenyl)-2-pyridylmethanethiolate(1–)), exhibits broad substrate reactivity. The kinetics of the reactions with X = Et_3P and XO = Me_2SO, Ph_2SO, $(CH_2)_4SO$, Ph_3AsO, Ph_2SeO, and pyridine N-oxide and three substituted variants have been measured in DMF solutions at 298 K. Activation parameters were determined for seven substrates over temperature ranges of at least 40 K including 298 K. All reactions follow second-order kinetics. In contrast to a previous analogue reaction system, kinetics parameters for reduction are sensitive to substrate. These were selected to cover a range of X–O bond dissociation energies, basicities, and steric factors. For reduction of substrates without large steric impediments, rate constants and $\Delta H^{\ddagger}$ values cover a range of 2.2 to 1 × 10^{-4} M^{-1} s^{-1} and 9.9–14.2 kcal/mol, respectively. Activation entropies (–21 to –33 eu) are consistent with an associative transition state. Rates are controlled by substantial contributions of both $\Delta H^{\ddagger}$ and $T\Delta S^{\ddagger}$ to $\Delta G^{\ddagger}$; no one property of the reductant **3** or substrate XO can be demonstrated to dominate relative reaction rates. Principal contributions to the activation enthalpies include major structural rearrangement of **3** (necessitated by the structural differences between **3** and **2**) and substrate binding and stabilization of the rearranged form of **3** (**5**), which can act as an oxo acceptor with a minimum of further rearrangement. A reaction scheme is proposed in which a species [**5**···OX]‡ is the transition state. The extent of X–O bond weaking in this state cannot be discerned because $\Delta H^{\ddagger}$ values do not correlate convincingly with X–O bond energies.

Introduction

Our most recent research in biologically related oxomolybdenum chemistry has resulted in the development of an improved analogue reaction system[2,3] for the molybdenum oxotransferases.[4] These enzymes catalyze the overall reaction X + H_2O ⇄ XO + $2H^+$ + $2e^-$, resulting in the oxidation/reduction of substrate X/XO. In our initial work in this area, we offered the hypothesis that the actual substrate oxidation or reduction step involves oxygen atom (oxo) transfer from or to the catalytic molybdenum center.[5,6] Key experiments by Hille and Sprecher[7] have confirmed this pathway for xanthine oxidase. For enzymes that do not contain terminal Mo=S bonds, the oxo transfer hypothesis is represented by eq 1 in Figure 1. This is an example of primary oxygen atom transfer,[8] in which the oxidation state of the mediating metal center is changed by two units and neither reactant nor product is a binuclear μ-oxo species.

The analogue reaction system of current interest is set out in Figure 1. It is based on the bidentate ligand *t*BuL-NS$^-$ (bis(4-*tert*-butylphenyl)-2-pyridylmethanethiolate(1–)), readily obtained as the lithium salt **1**.[3] Distorted octahedral $Mo^{VI}O_2$ complex **2** is easily prepared from **1** in high yield, and distorted trigonal bipyramidal $Mo^{IV}O$ complex **3** is derived from **2** by reductive oxo transfer using Et_3P.[3] This system has several advantages compared to our original system comprised of the complexes MoO_2(L-NS$_2$)/MoO(L-NS$_2$)(DMF).[6] Principal among these are a structurally authenticated $Mo^{IV}O$ complex,

ANALOGUE REACTION SYSTEM

$Mo^{VI}O_2$(*t*BuL-NS)$_2$ + X ⇌ $Mo^{IV}O$(*t*BuL-NS)$_2$ + XO (1)

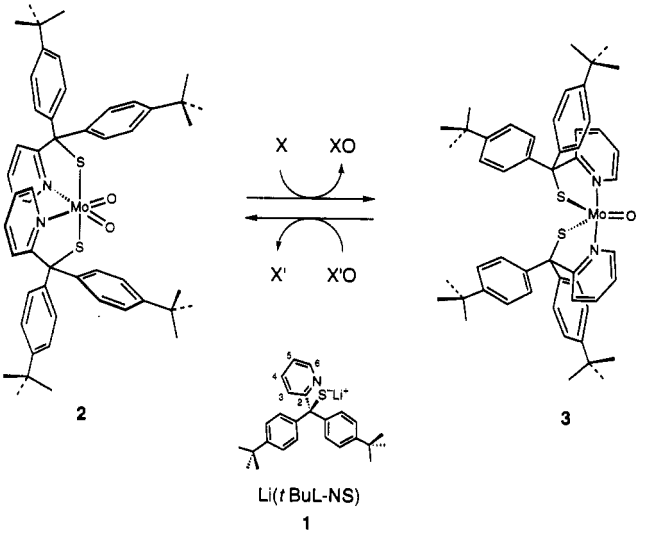

Figure 1. Depiction of an improved analogue reaction system based on MoO_2(*t*BuL-NS)$_2$ (**2**) and MoO(*t*BuL-NS)$_2$ (**3**), derived from ligand **1**. The structures of **2** and **3** have been determined by X-ray crystallography.[3]

stability to and reactivity with a much broader range of substrates, and sensitivity of reaction rates to the nature of the substrate. With use of ^{18}O labeling, it has been demonstrated that the atoms transferred to or from substrate must arise from the $Mo^{VI}O_2$ complex and XO, respectively. Further, the steric properties of **2** and **3** are such that the binuclear μ-oxo Mo(V) complex derivable from them does not form in polar solvents in the concentration range employed for reactivity studies.[9]

® Abstract published in *Advance ACS Abstracts*, September 1, 1993.

(1) National Science Predoctoral Fellow, 1989–1992.

(2) Gheller, S. F.; Schultz, B. E.; Scott, M. J.; Holm, R. H. *J. Am. Chem. Soc.* **1992**, *115*, 6934.
(3) Schultz, B. E.; Gheller, S. F.; Muetterties, M. C.; Scott, M. J.; Holm, R. H. *J. Am. Chem. Soc.* **1993**, *115*, 2714.
(4) Bray, R. C. *Q. Rev. Biophys.* **1988**, *21*, 299.
(5) Holm, R. H.; Berg, J. M. *Acc. Chem. Res.* **1986**, *19*, 363.
(6) Holm, R. H. *Coord. Chem. Rev.* **1990**, *100*, 183. The biologically related oxo-molybenum work of this laboratory prior to the development of the reaction system in Figure 1 is summarized here. L-NS$_2$ = 2,6-bis(2,2-diphenyl-2-sulfidoethyl)pyridine(2–).
(7) Hille, R.; Sprecher, H. *J. Biol. Chem.* **1987**, *262*, 10914.
(8) Holm, R. H. *Chem. Rev.* **1987**, *87*, 1401.
(9) The presence of such a species complicates the kinetics analysis of reaction 1 when monitored spectrophotometrically: (a) Reynolds, M. S.; Berg, J. M.; Holm, R. H. *Inorg. Chem.* **1984**, *23*, 3057. (b) Unoura, K.; Kato, Y.; Abe, K.; Iwase, A.; Ogino, H. *Bull. Chem. Soc. Jpn.* **1991**, *64*, 3372. A formal solution to this problem has been provided in ref a.

0020-1669/93/1332-4244$04.00/0

Table I. Activation Parameters for Mo-Mediated Oxo Transfer Reactions

reacn system[a]	solvent	$\Delta H^{\ddagger}$ (kcal/mol)	$\Delta S^{\ddagger}$ (eu)	ref
Substrate Reduction				
1. $MoO(L\text{-}NS_2)(DMF)$ + 3-FpyO	DMF	23.4(1.4)	7.2(2.0)	10
2. $MoO(L\text{-}NS_2)(DMF) + (R_F)_2SO$	DMF	22.1(1.3)	2.6(1.6)	10
3. $MoO(L\text{-}NS_2)(DMF) + NO_3^-$	DMF	23.7(6)	8(2)	11
4. $MoO[HB(Me_2pz)_3][S_2P(OEt)_2]$ + Me_2SO	PhMe	15.3(2)	−29(2)	12
Substrate Oxidation				
5. $MoO_2(L\text{-}NS_2) + (R_F)_3P$	DMF	11.7(0.6)	−28.4(1.6)	10
6. $MoO_2(ssp)(DMF) + EtPh_2P$	DMF	15.6	−20.7	13
7. $MoO_2(sap)(DMF) + EtPh_2P$	DMF	16.8	−19.7	13
8. $MoO_2(L\text{-}Cys\text{-}OEt)_2 + Ph_3P$	C_6H_6	11	−37	14

[a] Ligand abbreviations: $L\text{-}NS_2$ = 2,6-bis(2,2-diphenyl-2-sulfidoethyl)pyridine(2−); 3-FpyO = 3-fluoropyridine *N*-oxide; R_F = $p\text{-}C_6H_4F$; Me_2pz = 3,5-dimethylpyrazolyl; ssp = 2-(salicylideneamino)benzenethiolate(2−); sap = 2-(salicylideneamino)phenolate(2−).

While the initial system was most useful in demonstrating molybdenum-mediated oxo transfer with certain substrates, including several enzymatic substrates, its kinetics were uninformative with respect to the oxo transfer process itself. Summarized in Table I are all reported activation parameters for molybdenum-based oxo transfer.[10-14] Such data are limited, as in the case for metal-mediated oxo transfer reactions in general.[15] Note that systems 1–3, specific cases of our initial system, have experimentally indistinguishable activation enthalpies, similar activation entropies, and, consequently, essentially identical rate constants (k_1 = (1.4–1.6) × 10^{-3} s^{-1} at 298 K). These reactions proceed by binding of substrate followed by intramolecular first-order atom transfer. The difference of *ca.* 15 kcal/mol in the X–O bond dissociation energies of *N*-oxide and *S*-oxide substrates[16] is evidently not expressed to any detectable extent in the activation enthalpies. The data suggest a very early transition state or a structural rearrangement prior to (or perhaps concomitant with) oxo transfer. Initial studies of the reaction system in Figure 1 indicated that reaction rates were sensitive to substrate.[2] This has encouraged the more extensive kinetics examination of reaction 1 which is reported here. While our results do not permit identification of a unique reaction pathway, they do constitute the first comprehensive study of oxo transfer kinetics at any metal center with a variety of substrates. In addition to the determination of kinetics data, this work emphasizes the properties of complex and substrate that require consideration in any analysis of oxo transfer rates.

Experimental Section

Preparation of Compounds. The complexes $MoO_2(t\text{BuL-NS})_2$ and $MoO(t\text{BuL-NS})_2$ were prepared as described.[3] The substrate compounds 3-fluoropyridine *N*-oxide,[17] 2,6-diphenylpyridine *N*-oxide,[18] and diphenyl selenoxide[19] were synthesized by literature procedures. Pyridine (Fisher) was distilled from CaH_2 under dinitrogen and was degassed prior to use. Dimethyl sulfoxide (Fisher), HMPA (Aldrich), 2,6-lutidine *N*-oxide (Aldrich), and tetramethylene sulfoxide (Fluka) were distilled from CaH_2 under reduced pressure. Pyridine *N*-oxide was purified by vacuum sublimation. Diphenyl sulfoxide (Fisher) was recrystallized from benzene/hexane. Triphenylarsine oxide (Strem) and triethylphosphine (Aldrich) were used as received. Benzene and THF were distilled from sodium/benzophenone ketyl. Anhydrous DMF (99+%, Aldrich), the solvent for kinetics studies, was stored over 3–4 Å molecular sieves (Linde) and was degassed prior to use.

Table II. Kinetics Data for Oxo Transfer Reactions in DMF Solutions

XO/X	k_2 (298 K) (M^{-1} s^{-1})	$\Delta H^{\ddagger}$ (kcal/mol)	$\Delta S^{\ddagger}$ (eu)	$D_{X\text{-}O}$ (kcal/mol)	pK_{BH^+}
Et_3P	5.6(1) × 10^{-3}	9.6(6)	−37(2)		
Me_2SO	1.01(2) × 10^{-4}	13.6(2)	−31(1)	87	−1.80[d]
Ph_2SO	3.14(4) × 10^{-4}	14.2(5)	−27(2)	89	−2.54[d]
	1.44(2) × 10^{-3}	11.5(2)	−33(1)	(87)[a]	−1.34[e]
Ph_3AsO	5.6(2) × 10^{-2}	10.6(4)	−29(2)	103	0.99[f]
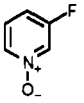	6.5(3) × 10^{-2}	9.9(2)	−31(1)	(72)[b]	(0.79)[b,g]
Ph_2SeO	2.16(6)	10.6(4)	−21(2)	(43)[c]	0.35[f]

[a] Value for Me_2SO. [b] Value for pyridine *N*-oxide. [c] See text. [d] Reference 21. [e] Reference 22. [f] Reference 23. [g] Reference 24.

Kinetics Measurements. Reactions were performed under strictly anaerobic conditions in DMF solutions. Reactions were monitored with a Varian spectrophotometer equipped with a cell compartment thermostated to ±0.5 °C. Substrate reduction reactions were followed by observing the disappearance of the 700-nm band of $MoO(t\text{BuL-NS})_2$. The oxidation of Et_3P was monitored by the decrease in intensity of the 371-nm feature of $MoO_2(t\text{BuL-NS})_2$. Sharp isosbestic points at 341 and 404 nm demonstrated that the reactions proceeded cleanly. Reaction systems contained the initial concentrations $[MoO_2(t\text{BuL-NS})_2]_0$ = 0.59–0.61 mM or $[MoO(t\text{BuL-NS})_2]_0$ = 1.7–2.5 mM and 10–1000 equiv of substrate, depending on reaction rates. For each substrate, reactions were run at four temperatures in the range 258–298 or 278–328 K. At each temperature, at least four runs were performed under pseudo-first-order conditions. Plots of $\ln[A/A_0]$ vs time ($Mo^{IV}O \rightarrow Mo^{VI}O_2$) or $\ln[A - A_\infty]/[A_0 - A_\infty]$ vs time ($Mo^{VI}O_2 \rightarrow Mo^{IV}O$) were linear over 3 half-lives. Linear plots of k_{obs} vs substrate concentration yielded the second-order rate constants k_2, which were used to determine activation parameters by means of Eyring plots. Errors were estimated using linear least-squares error analysis, with uniform weighting of the data points.[20] Weighting the data points individually did not change the errors appreciably. Reactions in solvents other than DMF were conducted and monitored similarly.

Results and Discussion

In the analogue reaction system of Figure 1, the forward reaction has been achieved with X = Et_3P and the reverse reaction with X′O = *S*-oxide, *Se*-oxide, *As*-oxide, nitrones and a variety of additional *N*-oxides including those of pyridine, other heterocyclic amines, and tertiary amines.[3] Substrate oxidation and reduction reactions are readily monitored spectrophotometrically owing to the distinct UV/visible absorption spectra of $MoO_2(t\text{BuL-NS})_2$ and $MoO(t\text{BuL-NS})_2$, which have been given elsewhere.[3] In substrate reduction, the bands of $MoO(t\text{BuL-NS})_2$ at 328, 430, 518, and 700 nm in DMF solution decrease in intensity and the single feature at 371 nm due to $MoO_2(t\text{BuL-NS})_2$ grows in. As the latter complex does not absorb appreciably in the visible region, substrate reduction can be followed by observing the change in intensity of the 700-nm band of $MoO(t\text{BuL-NS})_2$. In substrate oxidation, the single peak of $MoO_2(t\text{BuL-NS})_2$ grows in. Spectra measured over the course of substrate reduction and oxidation have been presented.[3] Reactions were conducted under pseudo-first-order conditions. In all cases, plots of $\ln(A/A_0)$ (substrate reduction) or of $\ln(A - A_\infty)/(A_0 - A_\infty)$ (substrate oxidation) vs time were linear over at least 3 half-lives. Plots of

(10) Caradonna, J. P.; Reddy, P. R.; Holm, R. H. *J. Am. Chem. Soc.* **1988**, *110*, 2139.
(11) Craig, J. A.; Holm, R. H. *J. Am. Chem. Soc.* **1989**, *111*, 2111.
(12) Roberts, S. A.; Young, C. G.; Cleland, W. E., Jr.; Ortega, R. B.; Enemark, J. H. *Inorg. Chem.* **1988**, *27*, 3044.
(13) Topich, J.; Lyon, J. T., III *Inorg. Chem.* **1984**, *23*, 3202.
(14) Deli, J.; Speier, G. *Transition Met. Chem.* **1981**, *6*, 227.
(15) For the remaining oxo transfer activation parameter data *cf.*: (a) Roecker, L.; Dobson, J. C.; Vining, W. J.; Meyer, T. J. *Inorg. Chem.* **1987**, *26*, 779. (b) Marmion, M. E.; Leising, R. A.; Takeuchi, K. J. *J. Coord. Chem.* **1988**, *19*, 1. (c) Rajapakse, N.; James, B. R.; Dolphin, D. In *New Developments in Selective Oxidation*; Centi, G., Trifiro, F., Eds.; Elsevier: Amsterdam, 1990; pp 109–117.
(16) Holm, R. H.; Donahue, J. P. *Polyhedron* **1993**, *12*, 571.
(17) Bellas, M.; Suschitzky, N. *J. Chem. Soc.* **1963**, 4007.
(18) Carde, R. N.; Hayes, P. C.; Jones, G.; Cliff, C. J. *J. Chem. Soc., Perkin Trans. 1* **1981**, 1132.
(19) Krafft, F.; Vorster, W. *Chem. Ber.* **1893**, *26*, 2820.
(20) Taylor, J. R. *An Introduction to Error Analysis*; University Science Books: Mill Valley, CA, 1982.

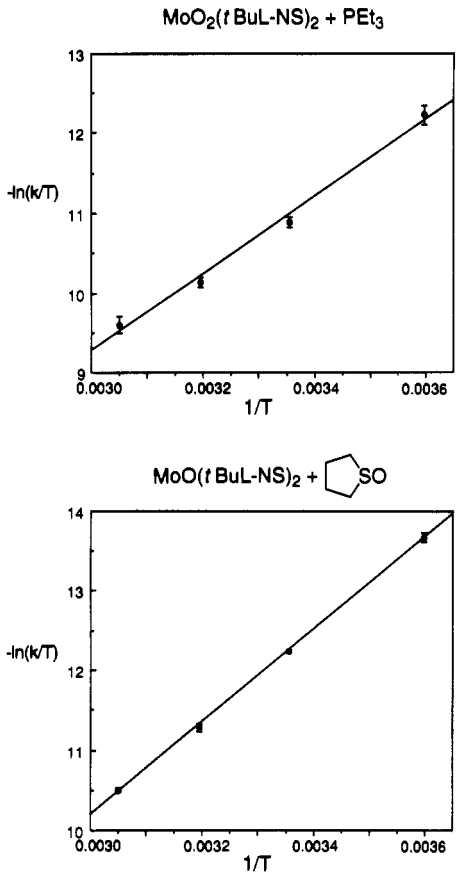

Figure 2. Eyring plots for oxo transfer reactions in DMF solutions at 278–328 K: (Top) oxidation of Et_3P by $MoO_2(t\text{BuL-NS})_2$; (bottom) reduction of $(CH_2)_4SO$ by $MoO(t\text{BuL-NS})_2$.

pseudo-first-order rate constants vs substrate concentration were linear for all substrates, demonstrating overall second-order reactions.

Kinetics data for seven substrates are compiled in Table II together with X–O bond dissociation energies[16] and basicity parameters,[21–24] which are considered subsequently. Activation parameters were calculated from the Eyring eq 2 utilizing rate constant data over a 40 or 50 K interval. Given that the rate constants at 298 K span a range of 10^4, it is evident that the kinetics data have the desired property of being substrate-dependent.

$$k = (k_B T/h)[\exp(-\Delta H^*/RT)\exp(\Delta S^*/R)] \quad (2)$$

Substrate Oxidation. Reaction 3, the preparative method for $MoO(t\text{BuL-NS})_2$,[2,3] was kinetically characterized; data are

$$MoO_2(t\text{BuL-NS})_2 + Et_3P \rightarrow MoO(t\text{BuL-NS})_2 + Et_3PO \quad (3)$$

$$d[MoO_2(t\text{BuL-NS})_2]/dt = -k_2[MoO_2(t\text{BuL-NS})_2][Et_3P] \quad (4)$$

included in Table II. The reaction follows the second-order rate law 4; its integrated form is given elsewhere.[25] The Eyring plot for this reaction is displayed in Figure 2. The large negative activation entropy is consistent with an associative mechanism.

Table III. Solvent Dependence of the Reaction Rates of $MoO(t\text{BuL-NS})_2 + (CH_2)_4SO$ at 298 K

solvent	k_2 (M^{-1} s^{-1})	ϵ^a	donor no.[b]
HMPA	$7.9(3) \times 10^{-4}$	29.6	38.8
DMF	$1.44(2) \times 10^{-3}$	36.7	24.0
pyridine	$2.82(8) \times 10^{-3}$	12.3	33.1
THF	$5.4(1) \times 10^{-3}$	7.32	20.0
benzene	$7.5(1) \times 10^{-3}$	2.28	0.1

[a] Dielectric constant. [b] Reference 32.

Table IV. Steric Inhibition of Reaction Rates for the Reduction of Pyridine *N*-Oxides by $MoO(t\text{BuL-NS})_2$ in DMF Solutions at 298 K

N-Oxide	k_2 (M^{-1} s^{-1})	pK_{BH^+}
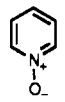	$3.04(5) \times 10^{-1}$	0.79[a]
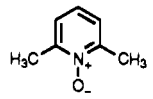	$4.3(2) \times 10^{-3}$	1.02[b]
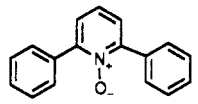	$4.3(3) \times 10^{-5}$	

[a] Reference 24. [b] Reference 23.

As in our previous reaction system,[10] we consider a feasible reaction pathway to involve interaction of the phosphine nucleophile with the vacant π^* orbitals of the $Mo^{VI}O_2$ group followed by development of a transition state with $Mo^{IV}{=}O$ character and concomitant Mo–O bond weakening and incipient P–O bond formation. The rate constants and activation parameters are similar to those of related systems (5–8, Table I). $MoO_2(t\text{BuL-NS})_2$ is also reduced by Ph_3P but much more slowly than in reaction 3; kinetics were not determined. With regard to enzymatic substrates whose kinetics would be of interest, sulfite (sulfite oxidase) effected slow decomposition of $MoO_2(t\text{BuL-NS})_2$,[3] and purines (xanthine oxidase) and aldehydes (aldehyde oxidase) require the $Mo^{VI}OS$ enzyme state, the analogue of which we have not been able to isolate in complexes based on ligand **1**.[26]

Substrate Reduction. Kinetics data for six substrates X′O in the substrate reduction reaction of Figure 1 have been determined and are presented in Table II. The reactions are described by the rate eq 5. An Eyring plot for the reduction of $(CH_2)_4SO$ is

$$d[MoO(t\text{BuL-NS})_2]/dt = -k_2[MoO(t\text{BuL-NS})_2][X'O] \quad (5)$$

given in Figure 2. This plot is entirely typical and illustrates well-behaved kinetics over the 278–328 K temperature interval. The relatively large negative activation entropies encountered in each case indicate an associative transition state. Solvent effects on the rates of the reduction of $(CH_2)_4SO$ are reported in Table III, and reaction rates of pyridine *N*-oxides with different extents of steric hindrance are listed in Table IV. Substrates were chosen to encompass a range of X′–O bond energies and basicities consonant with spectrophotometrically measurable reaction rates. In addition to these considerations, substrates were selected on other grounds. Dimethyl sulfoxide, tetramethylene sulfoxide, and pyridine *N*-oxide are enzyme substrates.[27] Tetramethylene

(21) (a) Landini, D.; Modena, G.; Scorrano, G.; Taddei, F. *J. Am. Chem. Soc.* **1967**, *91*, 6703. (b) Scorrano, G. *Acc. Chem. Res.* **1973**, *6*, 132.
(22) Curci, R.; Furia, F. D.; Levi, A.; Lucchini, V.; Scorrano, G. *J. Chem. Soc., Perkin Trans. 2* **1975**, 341.
(23) Klofutar, C.; Krasovec, F.; Kusar, M. *Croat. Chim. Acta* **1968**, *40*, 23.
(24) Jaffe, H.; Doak, G. O. *J. Am. Chem. Soc.* **1955**, *77*, 4441.
(25) Berg, J. M.; Holm, R. H. *J. Am. Chem. Soc.* **1985**, *107*, 925.
(26) The $Mo^{VI}OS$ functional group has been prepared in a perturbed form, but its reactivity toward enzyme substrates has not been reported: Eagle, A. A.; Laughlin, L. J.; Young, C. G.; Tiekink, E. R. T. *J. Am. Chem. Soc.* **1992**, *114*, 9195.
(27) (a) Satoh, T.; Kurihara, F. N. *J. Biochem. (Tokyo)* **1987**, *102*, 191. (b) Weiner, J. H.; MacIsaac, D. P.; Bishop, R. E.; Bilous, P. T. *J. Bacteriol.* **1988**, *170*, 1505. (c) McEwan, A. G.; Ferguson, S. J.; Jackson, J. B. *Biochem. J.* **1991**, *274*, 305.

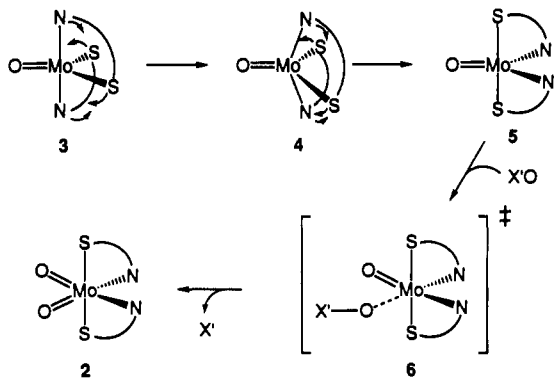

Figure 3. Schematic representation of a reaction pathway for the reduction of X'O by MoO(*t*BuL-NS)$_2$ (**3**). The steps include pseudorotation of **3** to **5**, which interacts with substrate to form transition state **6**; the latter passes to products MoO$_2$(*t*BuL-NS)$_2$ (**2**) and X' with a minimum of further rearrangement.

sulfoxide is less sterically hindered toward atom transfer than Me_2SO or Ph_2SO. Triphenylarsine oxide has the largest experimentally determined X'–O bond energy of any X'O compound we have found to be reduced in reaction 1. 3-Fluoropyridine *N*-oxide (3-FpyO) is a substrate common to our previous[10] and present[3] reaction systems. Diphenyl sulfoxide and diphenyl selenoxide are two structurally related substrates with substantial X'–O bond energy differences. 2,6-Lutidine *N*-oxide and 2,6-diphenylpyridine *N*-oxide present different extents of steric hindrance to atom transfer. In sharp contrast to the previous substrate reduction systems (1–3, Table I), rate constants and activation enthalpies are clearly dependent on substrate type.

Rates are controlled by an interplay of $\Delta H^{\ddagger}$ and $T\Delta S^{\ddagger}$ contributions. The latter is roughly constant and ranges from 36% to 48% of $\Delta G^{\ddagger}$; consequently, we examine those factors that potentially contribute to $\Delta H^{\ddagger}$ and influence relative rates of reaction.

(a) Structural Reorganization. With reference to the (idealized) structural depictions in Figure 1, it is evident that conversion of MoO(*t*BuL-NS)$_2$ to MoO$_2$(*t*BuL-NS)$_2$ involves substantial ligand rearrangement. If the incoming oxo atom were to be inserted in the equatorial plane of MoO(*t*BuL-NS)$_2$ cis to the Mo^{IV}=O group with no further structural change, the resultant six-coordinate species would have the cis,trans,cis $MoO_2N_2S_2$ arrangement rather than cis,cis,trans. This is a high-energy stereochemistry inasmuch as $Mo^{VI}O_2$ complexes invariably place two anionic (non-oxo) ligands trans and two neutral ligands cis.[28] Presumably for this reason, the actual stereochemistry of MoO$_2$(*t*BuL-NS)$_2$ is conventional. In the equatorial plane of MoO(*t*BuL-NS)$_2$ the bond angles S–Mo–S = 124.3(1)° and S–Mo–O = 118° (mean value), while the trans angle N–Mo–N = 160.5(3)°. Upon passage to the final configuration of MoO$_2$(*t*BuL-NS)$_2$, the following angle changes are required: +36° in S–Mo–S, –(17–28°) in S–Mo–O, and –84° in N–Mo–N. There are also small changes in Mo–ligand distances. A possible pathway for the required structural change is depicted in Figure 3. Initial complex **3** undergoes pseudorotation via trans square-pyramidal **4** to trigonal bipyramidal **5**, which is configured so as to facilitate oxo transfer with a minimum of additional ligand rearrangement. That **3** and not **5**, which requires relatively little ligand rearrangement, is the product of reaction 3 indicates that the former is the thermodynamically stable form of MoO(*t*BuL-NS)$_2$. Structural reorganization must contribute to the activation enthalpy. Given the large changes involved and weak substrate binding (vide infra), we conclude that this contribution to $\Delta H^{\ddagger}$ is unlikely to be significantly dependent on substrate.

(28) There is only one exception to this stereochemical regularity, and it is forced by steric interactions: Dreisch, K.; Andersson, C.; Stålhandske, C. *Polyhedron* **1992**, *11*, 2143; **1993**, *12*, 303.

(b) Bond Strengths. Bond dissociation energies of substrates X'O are readily evaluated from ΔH for the reaction X(g) + $^1/_2O_2$(g) → XO(g) and the dissociation energy of O_2(g). Values are tabulated elsewhere.[16] If in the transition state there is substantial X'–O bond stretching or incipient dissociation, this situation should be expressed as a contribution to the activation enthalpy. The *dominance* of this effect would afford an order of activation enthalpies which correlates with bond strengths. Of the substrates in Table II, three bond energies can be directly evaluated from thermodynamic data while three others are approximate values necessarily assigned from other compounds. The assignment of the value for Me_2SO to $(CH_2)_4SO$ is acceptable given that S–O bond energies in dialkyl and diaryl sulfoxides occur in a very narrow range.[16,29] The value for 3-FpyO is approximated by the value for pyridine *N*-oxide. Thermodynamic data necessary to the evaluation of the Se–O bond energy of any organo selenoxide are unavailable. The only value available is that for $SeOCl_2$ (58 kcal/mol).[16] If the difference in bond energies is the same for the pair $SeOCl_2/Ph_2SeO$ as for $SOCl_2/Ph_2SO$ (15 kcal/mol), the bond energy of Ph_2SeO is estimated as 43 kcal/mol. These uncertainties notwithstanding, it is probable that the Se–O bond in Ph_2SeO is weaker than the S–O bond in Ph_2SO by *ca.* 35–45 kcal/mol.

The data in Table II reveal that rate constant and $\Delta H^{\ddagger}$ data do not uniformly correlate with D_{X-O} values. There is a correlation over the substrate set in the order R_2SO < 3-FpyO < Ph_2SeO, but Ph_3AsO, whose bond energy is derived from recent thermochemical data,[16,30] has a rate constant about 40–550 times larger than the three sulfoxides. Further, this substrate, which has the *largest* bond energy (103 kcal/mol), manifests $\Delta H^{\ddagger}$ = 10.6(4) kcal/mol, indistinguishable from that of Ph_2SeO, which has the *smallest* bond energy. The probable difference in these D_{X-O} values is *ca.* 50 kcal/mol. While Ph_2SeO reacts much more rapidly than Ph_3AsO, this effect is due to the most favorable activation entropy of any reaction.

(c) Solvent Effects. Five solvents covering a significant range of dielectric constant and coordinating ability as measured by the donor number concept were selected. Rate constants at 298 K for the reduction of $(CH_2)_4SO$, employed because of its convenient reaction rates, are set out in Table III. In each solvent, the absorption spectrum of MoO(*t*BuL-NS)$_2$ remained qualitatively the same, with only slight shifts of band maxima. Tight isosbestic points were maintained. These results argue against any major structural difference in these solvents.[31] The observed rate constants differ maximally by a factor of 9.4, corresponding to 1.3 kcal/mol in $\Delta G^{\ddagger}$. The slowest and fastest reactions occur in those solvents with the largest (HMPA) and smallest (benzene) donor numbers.[32] However, the rates do not correlate with donor number or with dielectric constant in HMPA and DMF. The reaction in benzene is only 2.7 times faster than that in related but potentially coordinating solvent pyridine. Such small differences, combined with spectral similarities and parallel trends in rate constant and dielectric constant in pyridine, THF, and benzene, lead to the suggestion that solvent effects on reaction rates derive mainly from solvation energy differences in the various solvents rather than from competitive binding of solvent.[33] In addition, large excesses of tetrahydrothiophene and *t*-BuNC did not perturb the ^{1}H NMR spectrum of MoO(tBuL-NS)$_2$ in

(29) Herron, J. T. In *The Chemistry of Sulfones and Sulfoxides*; Patai, S., Rappaport, Z., Stirling, C. J. M., Eds.; Wiley: New York, 1988; Chapter 4.

(30) Barnes, D. S.; Burkinshaw, P. W.; Mortimer, C. T. *Thermochim. Acta* **1988**, *131*, 107.

(31) Reactions in all solvents in Table III were conducted in concentration ranges such that no appreciable concentration of the μ-oxo species [MoO(*t*BuL-NS)$_2$]$_2$O was present. We have reported the formation of this complex in concentrated benzene solutions.[3]

(32) Gutmann, V. *The Donor-Acceptor Approach to Molecular Interactions*; Plenum Press: New York, 1978; Chapter 2.

benzene, indicating that the complex remains five-coordinate under these conditions.

Of all potential ligands tested, only Me_3P gave a positive indication. Addition of excess phosphine to MoO(*t*BuL-NS)$_2$ in benzene resulted in a color change from brown to deep red-violet and replacement of a single 6-H resonance (Figure 1) at 9.4 ppm with two equally intense peaks at 8.3 and 10.5 ppm. These results are indicative of a major structural change in which the endogenous ligand binds cis to the oxo ligand, thereby breaking the C_2 symmetry of the unligated complex.[34]

(d) Basicity and Binding. The five-coordinate structure of MoO(*t*BuL-NS)$_2$ in either configuration **3** or **5** would appear to allow substrate binding to the molybdenum atom cis to the oxo ligand in the equatorial plane. However, given the structure of **2**, binding productive to atom transfer is restricted to **5**. If the substrate binds in a pre-equilibrium step 6, the ability of substrate

$$\underset{\mathbf{5}}{\mathrm{MoO}(t\mathrm{BuL\text{-}NS})_2} + \mathrm{X'O} \rightleftarrows \mathrm{MoO}(t\mathrm{BuL\text{-}NS})_2(\mathrm{X'O}) \quad (6)$$

to bind and stabilize the reorganized complex **5** may influence the transition-state energy and, hence, modify the reaction rate. This situation subsumes the possibility that substrate binding is rate-limiting inasmuch as the observed second-order kinetics do not permit a distinction. In these circumstances, the transition state would resemble the product adduct of reaction 6. Although these substrate types form numerous metal complexes, the only available means of reducing their intrinsic nucleophilicities to a common scale is by comparison of basicity constants pK_{BH}^+. Values in Table II were measured using different techniques and different assumptions concerning the use of acidity functions. Because of this and because proton affinities do not necessarily parallel metal binding affinities, the data are useful only for defining the trend of increasing basicity[23] in series 7 (R = alkyl or aryl). Sulfoxides, the weakest bases, afford the highest $\Delta H^{\ddagger}$

$$\mathrm{R_2SO} < \mathrm{R_2SeO} < \mathrm{pyO} < \mathrm{R_3AsO} \quad (7)$$

values, while 3-FpyO and Ph_3AsO, the two strongest bases, are associated with the lowest $\Delta H^{\ddagger}$ values. Activation enthalpies of Ph_3AsO and Ph_2SeO are indistinguishable, a result consistent with the relatively small difference in basicity constants. Again, the former substrate reacts faster because of a larger $\Delta S^{\ddagger}$ value, the origin of which is unclear. The trend relating $\Delta H^{\ddagger}$ and pK_{BH}^+ shows no major inconsistencies. Hence, it is probable that binding to and stabilization of rearranged complex **5** is a contributor to the activation enthalpies.

(e) Steric Factors. The rates of reaction of three pyridine bases with MoO(*t*BuL-NS)$_2$ in DMF solutions at 298 K are compared in Table IV. Clearly, steric factors significantly modulate the reaction rates. The reduction of 2,6-lutidine *N*-oxide is 10^2 slower than that of pyridine *N*-oxide. Molecular models indicate that the former is not sufficiently hindered to prevent binding to the molybdenum atom. The reduction of 2,6-diphenylpyridine *N*-oxide is some 10^4 times slower, indicating that the two phenyl groups do provide a major steric barrier. These experiments were performed primarily in an attempt to discern if initial attack by the substrate on the oxo group could occur, which, if operative, would result in a peroxide intermediate. Because of the outward projection of the Mo^{IV}–O bond, it would appear that extent of frontside hindrance of the *N*-oxides is not sufficient to account for very large rate decreases observed. While these are entirely qualitative considerations, we favor direct interaction of the substrate oxygen atom with the molybdenum atom.

Summary. This work presents the first extensive kinetics study of substrate reduction by oxygen atom transfer. The following are the principal results and conclusions of this investigation.

(1) Substrate oxidation and reduction in reaction 1 (Figure 1) proceed by second-order pathways; saturation kinetics, first-order oxo transfer, and rate constants and activation parameters insensitive to substrate in reduction reactions of previous systems[6,10,11,25] are not observed here.

The points below refer to substrate reduction.

(2) Analysis of relative rates of reduction is complicated by the appreciable (36–48%) contribution of $T\Delta S^{\ddagger}$ to $\Delta G^{\ddagger}$; no one property of the Mo^{IV}=O reductant or of substrate can be demonstrated to dominate the relative values of rate constants.

(3) Principal contributors to $\Delta H^{\ddagger}$ include structural reorganization, made apparent by the structural differences of MoO(*t*-BuL-NS)$_2$ (**3**) and MoO_2(*t*BuL-NS)$_2$ (**2**), and substrate binding and stabilization of the rearranged form of MoO(*t*BuL-NS)$_2$ (**5**). No convincing correlation of substrate bond energies and $\Delta H^{\ddagger}$ values emerges. Solvent effects on rates arise from differential solvation effects rather than competitive binding, and substrate steric effects on rates do not appear to be inconsistent with metal- rather than oxo-based attack.

(4) The scheme in Figure 3 provides a plausible description of the reaction pathway. Initial complex **3** converts by pseudorotation to **5**, which is subject to substrate binding and the formation of an associative transition state resembling **6**. Intramolecular atom transfer affords the products X′ and **2**. The extent of weakening of the X′–O bond in the transition state remains uncertain.

This work serves to point out the properties of substrate and complex that potentially affect the rates of atom transfer. Systems involving substantial ligand rearrangement are necessarily complicated in the sense that, if the influence of substrate properties on rate is sought, this may be only a relatively small fraction of the activation enthalpy. An optimal system for this purpose, currently unknown, is that exhibiting saturation kinetics and first-order atom transfer which itself is rate-determining.

Acknowledgment. This research was supported by National Science Foundation Grant CHE 92-08387. We thank Dr. S. F. Gheller and S. C. Lee for useful discussions.

(33) It might also be argued that if DMF and HMPA are good ligands toward MoO(*t*BuL-NS)$_2$, so would be $(CH_2)_4SO$. If this were true, saturation kinetics would be expected at high sulfoxide concentration. Inasmuch as second-order kinetics apply at [R_2SO]/[MoO(*t*BuL-NS)$_2$] ratios up to 1000:1, competitive binding of solvent is not responsible for the observed solvent effects on reaction rates.

(34) Despite numerous attempts with a variety of ligands including Me_3P, we have been unable to obtain diffraction-quality crystals of any ligated form of MoO(*t*BuL-NS)$_2$.